DESIGN STUDIES FOR AN UPGRADE OF THE SLS STORAGE RING

A. Streun, M. Aiba, M.Böge, M. Ehrlichman, Á. Saá Hernández, PSI, Villigen, Switzerland

Abstract

An upgrade of the Swiss Light Source (SLS) would replace the existing storage ring by a low aperture multibend achromat lattice providing an emittance of about 100–200 pm at 2.4 GeV, while maintaining the hall, the beam lines and the injector. Since emittance scales inversely cubically with the number of lattice cells, an SLS upgrade is challenged by the comparatively small ring circumference of only 288 m. A new concept for a compact low emittane lattice is based on longitudinal gradient bending magnets for emittance minimization and on anti-bends (i.e bends of opposite field polarity) to disentangle dispersion and horizontal beta function in order to provide the optimum matching to the longitudinal gradient bends while minimizing the contribution to chromaticity.

INTRODUCTION

The Swiss Light Source (SLS) is in user operation since 2001. The storage ring is a 12 triple bend achromat (TBA) lattice providing an equilibrium emittance of 5.0 nm at 2.4 GeV beam energy. SLS had to accommodate experiments covering a wide range of photon energies and polarizations, which resulted in a lattice layout with 3 different types of straights: 6×4 m, 3×7 m and 3×11.5 m. In 2005/06 the FEMTO insertion for laser-beam slicing and three 3 Tesla superbends were installed in order to provide sub-ps X-ray pulses and hard X-rays up to 45 keV. Today the SLS is fully equipped with 18 user beam lines and delivers about 5000 hours of user beam time per year at an availability of 97.3% (10 years average) [1].

In recent years, progress in technology and lattice design, mainly pioneered by the MAX IV project [2], introduced a generational change in the field of electron storage rings: multibend achromat (MBA) lattices based on the miniaturization of vacuum chambers and multipole magnets provide an increase of photon beam brightness by 1–2 orders of magnitude and a corresponding increase of spatial coherence. Thus, in a few years from now, the third generation lights sources may no longer be competitive with respect to most advanced experimental techniques like coherent imaging, ptychography, resonant inelastic X-ray scattering etc. So, like for many other facilities, an upgrade is considered for the SLS too. It is planned to replace the storage ring by a new one providing 100–200 pm emittance, while keeping the shielding walls, the beam line source points and the injector complex.

However, the circumference of the SLS is rather small compared to other machines, thus replacing the TBAs by MBAs alone will not provide the desired emittance: just scaling the lattice of MAX IV to the energy and size of SLS results in an emittance of about 1 nm, which would not justify a major upgrade. Also damping wigglers are precluded by lack of space.

A potential way out is based on a new type of lattice cell providing five times lower emittance, which will be presented in the next section. Design studies for an upgraded SLS based on this cell will be presented in the section after the next. The issues of dynamic aperture optimization, error sensitivity, injection schemes and possible round beam operation are treated elsewhere [3–6].

A NEW LOW EMITTANCE CELL

The Problem of the TME Cell

The minimum theoretical emittance (TME) ϵ^{TME} which can be provided by a gradient-free bending magnet of given deflection angle is well known [7], but a periodic and symmetric lattice cell which fulfills the matching conditions for the horizontal beta function β_{xo}^{TME} and the dispersion η_o^{TME} at the bend center, is of little practical use: the dispersion production of a bend is given by its curvature, $\eta'' = h = eB/p$, and acts like a defocusing force on the dispersion. Adjusting the horizontally focusing quadrupoles to match exactly the TME conditions for the dispersion *and* the beta function and finding a periodic solution, i.e. $\beta'_x = \eta' = 0$ a the cell ends, results in an over-focused beta-function and a very high horizontal betatron phase advance of 284.5°. The lattice cell thus needs a second focus in order to accommodate the excess betatron phase, so it becomes rather long and the optics is overstrained. As a consequence, only relaxed TME-cells are commonly used, where the cell phase advance is well below 180°, and the emittance is about a factor 3–6 larger than the TME. Defining dimensionless parameters

$$F = \epsilon/\epsilon^{\text{TME}} \qquad b = \beta_{xo}/\beta_{xo}^{\text{TME}} \qquad d = \eta_o/\eta_o^{\text{TME}}$$

elliptic iso-emittance contours $F(b, d)$ are obtained as shown in Fig. 1 (left) [8].

Construction of a low emittance cell with unstrained optics proceeds by two steps:

1. disentangle beta function and dispersion using anti-bends,

2. minimize emittance using longitudinal gradient bends.

Anti-bends

Anti-bends (AB), i.e. bends of negative field forming a star-shaped rather than a polygonal lattice have been considered in the 1980s and 90s for isochronous rings or for enhanced radiation damping ("wiggler lattice"). The potential for emittance reduction had been noticed [9] but was never exploited.
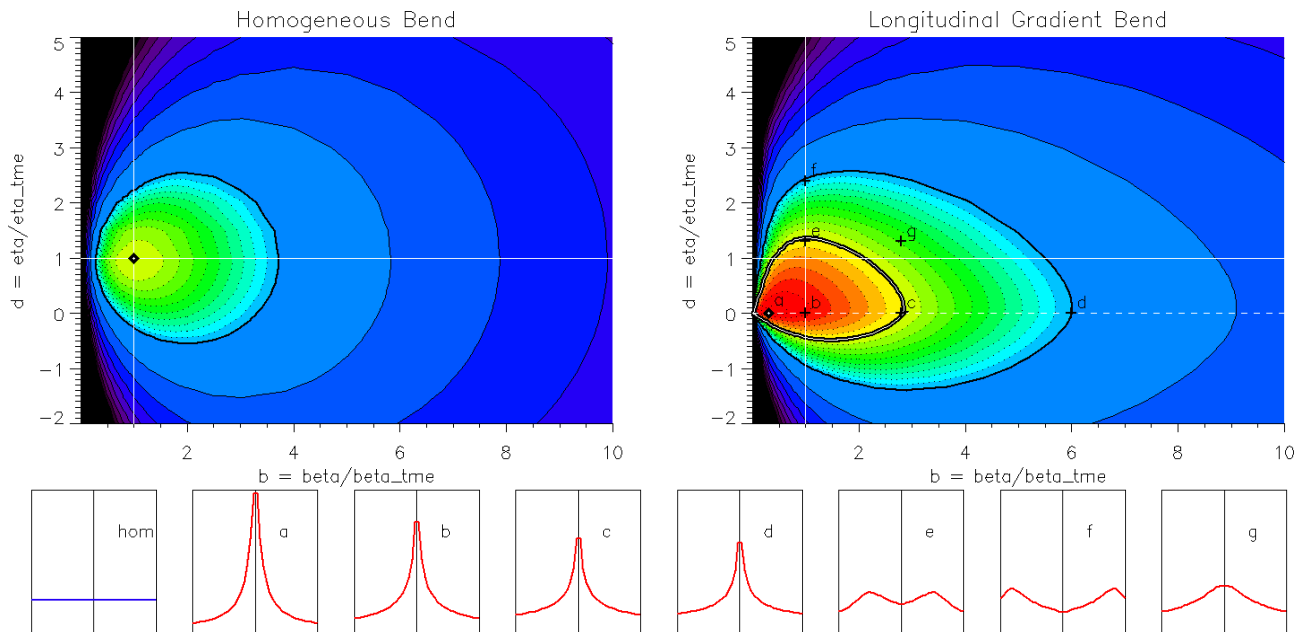
Figure 1: Contours of normalized emittance F vs. normalized beta function b and dispersion d for a homogeneous bend (left) and an optimized longitudinal gradient bend (right). The diamond symbol at (1,1) in the left plot and the double line in the right plot both correspond to the case $F = 1$, i.e. the TME emittance. The thick line corresponds to $F = 2$, the thin lines to $F = 3, 4, 5 \ldots$ The dotted lines are spaced by 0.1 in F. The diamond symbol in the right plot marks the minimum value of $F \approx 0.35$. The small figures at bottom show optimized longitudinal field profiles for various points (b, d) marked by characters in the right plot. Optimizations were done for a symmetric LGB of 8° deflection at 2.4 GeV and 0.8 m length.

An AB of angle $-\psi$ provides a kick to the dispersion function,

$$\Delta\eta' = -\psi,$$

which results in a reduction of the dispersion at the main bend center η_o, if the AB is out of phase with the main bend. Lowest emittance is obtained for a cell phase advance of about 160°. The beta functions are virtually not affected by the AB.

The AB deflection angle amounts to approx. -10% of the main bend angle, thus the main bend angle has to be increased correspondingly in order to maintain the total cell deflection. This diminishes the emittance reduction effect. Furthermore, the AB is located at a location of large dispersion and beta function, which is inconvenient with regard to emittance. Nevertheless, the net effect is a substantial emittance reduction by a factor 2–3 [10].

The AB contribution to the 5th radiation integral is approximately given by

$$I_5 = \int |h^3|\mathcal{H}\, ds \quad \xrightarrow{\text{AB}} \quad \approx \frac{\eta^2|\psi^3|}{\beta_x L^2}, \qquad (1)$$

because dispersion and beta function are approximately constant at its location (preview Fig. 2). ($\mathcal{H}$ is the betatron amplitude of the dispersion function.) Therefore the contribution to emittance is minimized making the AB rather long and weak.

Since the ABs are located at the cell ends (out of phase with the main bend), where the horizontal focusing is required, an AB may conveniently be built as a combined function magnet or even as a half-quadrupole as the most simple design. Like a vertical focusing gradient in a normal bend, the horizontal focusing gradient in the AB increases the horizontal damping partition number J_x hence further reducing the emittance.

Large dispersion at the ABs gives a large negative contribution to the momentum compaction factor α, overcompensating the positive contribution from the main bend, since dispersion – by means of the AB – has been adjusted to very small values there. For $\alpha < 0$ and negative chromaticity, the head-tail instability does not appear [11]. Since chromaticity is negative by nature, and its absolute value is modest due to unstrained horizontal focusing in the AB-based cell, the strength of the chromaticity correcting sextupoles can be reduced by substantial amount, thus alleviating the task of dynamic aperture optimization.

Longitudinal Gradient Bends

Longitudinal variation of a bend's field or curvature $h(s)$ to compensate the growth of the dispersion's betatron amplitude $\mathcal{H}(s)$ towards the endges of the bend minimizes the 5th radiation integral (see Eq. 1) and renders possible an emittance below the TME [12].

Figure 1 (right) shows the normalized emittance F as a function of the normalized optics parameters b and d. A numerical optimization of the field profile was done for each point in the (b, d) plane with the 5th radiation integral as the objective and constraints on bending angle and length. Examples of field profiles are shown at the bottom of Fig. 1.

The TME point $F = b = d = 1$ of the homogenous bend (left plot) opens up becoming a wide contour line, inside the emittance is smaller than the TME ($F < 1$), with a minimum of $F \approx 0.35$ at $d \approx 0$ and $b \approx 0.3$. The minimum is finite but depends on model parameters and on the LGB length, whereas the homogeneous bend's TME is independent from its length.
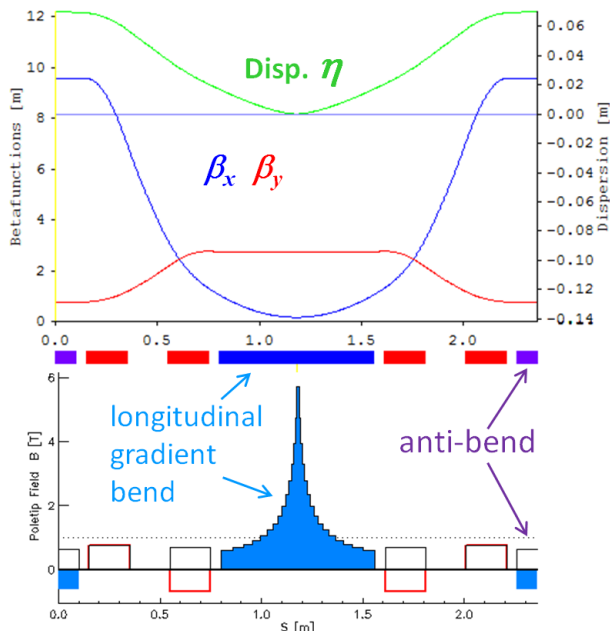

Figure 2: A lattice cell combining longitudinal gradient bends and anti-bends. Top plots shows the optics, bottom plot the magnet pole tip fields at an aperture radius of $R = 13$ mm: dipole field in blue, quadrupole in red, total in black. Parameters: 6.7° total deflection, 2.36 m length, phase advance hor./vert. 160°/ 90°, damping partition $J_x \approx 1$, emittance 200 pm at 2.4 GeV.

In view of lattice design it is most interesting to notice that low emittance from an LGB requires virtually zero dispersion at its center, but a modest beta function can be tolerated. Compared to the homogeneous bend, the TME value of emittance is obtained at almost three times larger beta function in the LGB. Hence, efficient use of the LGB requires dispersion and beta function to be disentangled by means of ABs [13].

Figure 2 shows the new LGB-AB-cell combining both magnet types: The ABs create approx. zero dispersion in the LGB center, where the hyperbolic field has a narrow, high peak. This cell provides an almost five times lower emittance ($F = 0.69$) than a relaxed TME cell ($F = 3.4$) of identical length, deflection and phase advances.

SLS UPGRADE LATTICE DESIGNS

Presently three draft designs are considered in parallel, one is a hybrid-MBA (HMBA) and two are of LGB-AB type. Figure 3 shows the optical functions and Table 1 gives the most important parameters. All lattices have a beam energy of 2.4 GeV, a circumference of 288 m and six short, three

medium and three long straight sections. Anticipating user demands, in lattices C and D the long straights are split into two short straights to allow canted undulators to be installed. Assuming a narrow NEG-coated beam pipe similar to the one used at MAX IV [14], a magnet aperture radius of 13 mm is assumed. Following ESRF magnet designs [15], poletip fields of quadrupoles, sextupoles and octupoles are limited to 1.05, 0.75 and 0.45 T.

Lattice A is based on a central 6 T super-LGB bracketed by the main chromaticity sextupoles in an approximate $(-I)$ transformer configuration. Small ABs support matching, apart from that the arc is rather conventional.

Lattices C and D are LGB-AB cell based, star-shaped MBAs of $> 500°$ total absolute deflection angle, which achieve a very low emittance at moderate chromaticity and negative momentum compaction. LGB peak field is 5 T in lattice C and 2 T in lattice D: higher field leads to shorter LGBs leaving more space for the straight sections, lower field provides lower radiation loss and energy spread.

The narrow high field peak of a super-LGB may provide hard X-rays (up to 100 keV at 2.4 GeV) while only little increasing radiation loss and energy spread.

Table 1: SLS Upgrade Lattice Designs

Name		A [ah04n]	C [ca06b]	D [db02a]
Type		HMBA	LGB-AB	LGB-AB
ϵ	[pm]	183	126	132
ν_x		39.4	37.7	38.1
ν_y		10.8	10.8	10.2
ξ_x		-163	-61	-70
ξ_y		-70	-49	-34
α	$[10^{-4}]$	$+1.29$	-1.00	-1.01
$\sigma_{\Delta E/E}$	$[10^{-3}]$	1.04	1.24	1.00
ΔE_{rad}	[keV]	466	735	544
L_{short}	[m]	3.2	3.6	2.9
L_{medium}	[m]	5.7	6.2	4.8
L_{long}	[m]	10.0	5.0 + 5.0	5.0 + 5.0

CONCLUSION & OUTLOOK

A lattice cell combining longitudinal gradient bends and anti-bends may provide an emittance of 100–200 pm at 2.4 GeV for the rather compact lattice of the SLS. Tentative designs are presently under consideration. Dynamic aperture optimizations [3] and injection design [5] are in progress, studies on instabilities due to interaction of the beam with the narrow vacuum chambers and on alignment and optics corrections [4] have been started. A conceptual design report is scheduled for the end of 2016.
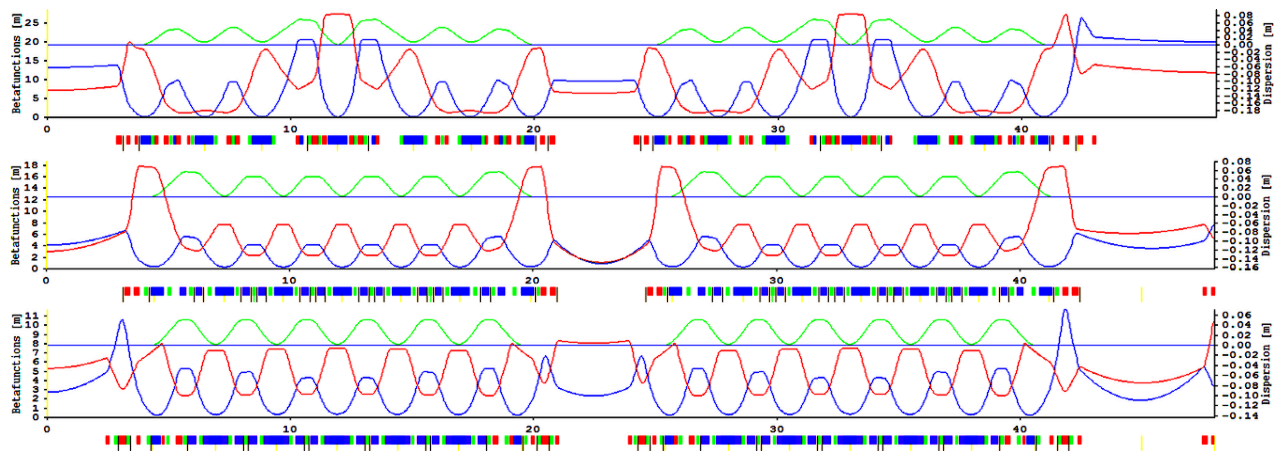
Figure 3: Three tentative SLS upgrade lattices A,C,D. One sixth of the ring is shown, i.e. half a super-period (β_x, β_y, η).

REFERENCES

[1] SLS Operation Statistics, http://www.psi.ch/sls/operation-statistics

[2] S.C. Leemann *et al.*, Phys. Rev. ST Accel. Beams 12, 020701 (2009).

[3] M. Ehrlichman, M. Aiba, and A. Streun, "Optimizing SLS-2 Nonlinearities using a Multi-Objective Genetic Optimizer", presented at IPAC'15, Richmond, VA, USA, May 2015, paper MOPJE074, these proceedings.

[4] M. Böge, M. Aiba, and A. Streun, "Orbit Correction and Stability Studies for Ultra-Low Emittance Storage Rings", presented at IPAC'15, Richmond, VA, USA, May 2015, paper TUPJE048, these proceedings.

[5] A. Saa Hernandez and M. Aiba, "Investigation of SLS2 Injection Scheme", presented at IPAC'15, Richmond, VA, USA, May 2015, paper TUPJE046, these proceedings.

[6] M. Aiba, M. Ehrlichmann, and A. Streun, "Round Beam Operation in Electron Storage Rings and generalisation of Mobius accelerator", presented at IPAC'15, Richmond, VA, USA, May 2015, paper TUPJE045, these proceedings.

[7] L.C. Teng, "Minimum emittance lattice for synchrotron radiation storage rings", ANL internal report LS-17 (1985).

[8] S.C. Leemann and A. Streun, Phys. Rev. ST Accel. Beams 14, 030701 (2011).

[9] J.P. Delahaye and J.P. Potier, "Reverse bending magnets in a combined function lattice for the CLIC damping ring", in *Proc. PAC'89*, Chicago, IL, USA, March 1989, p. 1611.

[10] A. Streun, Nucl. Instrum. Methods Phys. Res. A 737 (2014) 148–154.

[11] D. Robin *et al.*, "Experimental results on low alpha electron-storage rings", Micro bunches workshop, Upton, NY, USA, Sep. 1995.

[12] A. Wrulich, "Overview of 3rd generation light sources", Workshop on Fourth Generation Light Sources, SSRL/SLAC, Stanford, CA, USA, Feb. 1992.

[13] A. Streun and A. Wrulich, Nucl. Instrum. Methods Phys. Res. A 770 (2015) 98–112.

[14] E. Al-Dmour *et al.*, J. Synchrotron Rad. 21 (2014) 878–883.

[15] J. Chavanne *et al.*, "Magnets and insertion devices for the ESRF II", presented at Beam Dynamics meets Magnets II Workshop, Bad Zurzach, Switzerland, Dec. 2014.